Scanning Microscopy

Volume 6 | Number 2 Article 15

6-24-1992

Enamel Structure in Astrapotheres and Its Functional Implications

John M. Rensberger
University of Washington

Hans Ulrich Pfretzschner
University of Bonn

Scanning Microscopy, Vol. 6, No. 2, 1992 (Pages 495-510) 0891-7035/92$5.00+.00
Scanning Microscopy International, Chicago (AMF O'Hare), IL 60666 USA

ENAMEL STRUCTURE IN ASTRAPOTHERES AND ITS FUNCTIONAL IMPLICATIONS

John M. Rensberger* [1] and Hans Ulrich Pfretzschner[2]

[1]Department of Geological Sciences and Burke Memorial Washington State Museum, University of Washington, Seattle; [2]Institut für Paläontologie, University of Bonn, Bonn, Germany.

(Received for publication February 17, 1992, and in revised form June 24, 1992)

Abstract

Astrapotheres, large extinct ungulates of South America, share with rhinoceroses vertical prism decussation in the cheek tooth enamel. The similarity extends beyond merely the direction of the planes of decussation. The vertical decussation in astrapotheres is confined to the inner part of the enamel and has uniformly well-defined zones in which the prism direction differs by nearly 90° and the zones are separated by narrow transitional borders of intermediate prism direction. The outer enamel consists of predominantly occlusally and outwardly directed prisms. Within the outer enamel is a region of horizontally decussating prisms; here the angle of decussation is usually smaller than that of the inner vertically decussating prisms.

Except for the horizontal decussation in the outer enamel, these conditions match structures that have been described for rhinocerotoids. These features, together with the similarity in premortem crack direction and gross shape of the cheek teeth, imply that astrapotheres and rhinocerotoids shared essentially the same system of cheek tooth mechanics.

However, the microstructure of the canine enamel in the astrapotheres is distinct. The lower canine enamel of the Oligocene *Parastrapotherium* exhibits a form of vertical decussation modified by a wavelike bending of prism zones, whereas the decussation in the rhinocerotoid canine is horizontal. The lower canine in *Parastrapotherium* was subjected to different loading conditions, judging from multiple sets of premortem crack directions. The modified vertical decussation would in theory resist cracking under different directions of tensile stresses. This is confirmed by the sinuous paths of cracks that run in directions differing by up to 90°. That diverse stresses were generated in the enamel during life is confirmed by the pattern of premortem cracks in *Parastrapotherium*. The enamel in the upper canine of a late Miocene astrapothere lacks decussation but may have resisted cracking under varied loading conditions by virtue of a 3-dimensional wavelike bending of the prisms.

Key Words: Enamel microstructure, molar, canine, stresses, crack patterns, fracture resistance, functional morphology, convergent evolution, Astrapotheria, *Astrapotherium*, *Parastrapotherium*, Rhinocerotoidea.

*Address for correspondence:
Department of Geological Sciences
and Burke Memorial Washington State Museum
University of Washington DB-10
Seattle, Washington 98195
Phone No.: (206) 543-7036; FAX: (206) 543-9285

Introduction

Mammalian teeth have a great range of form and these differences have been used extensively to determine phyletic relationships and evolutionary histories. The dental diversity in mammals derives in part from the diversity of dental function and behavioral use of teeth, which include food gathering and processing, offensive and defensive behaviors as well as social activities (Crompton & Hiiemae, 1969).

It is well known that the microstructure of mammalian tooth enamel varies considerably among taxa (e.g. Korvenkontio, 1934, Kawai, 1955; Boyde, 1978). Recently, evidence has been found that differences in enamel microstructure in at least some taxa have not arisen randomly but somehow represent responses to selective factors in the chewing mechanics and dietary adaptations. A directional asymmetry of the enamel microstructure within single molars of arvicoline rodents is related to the direction of motion of the jaws during mastication (von Koenigswald, 1980). A reorientation of the microstructural fabric in tapiroids and rhinocerotoids, in which the occlusal surface has become highly lophodont, is related to the attitude of the functional edges of the lophs and hence to the masticatory mechanism (Rensberger & von Koenigswald, 1980; Fortelius, 1985; Boyde and Fortelius, 1986). Prism decussation is weak or absent in the soft food eating ceboid primate *Alouatta* but well developed in *Cebus apella*, *C. albifrons*, and *Chiropotes*, whose diets include hard objects (Maas, 1986). The directions of the prisms in the molars of the koala and in the opossum are related to the direction of the occlusal force (Young, et al., 1987; Stern, et al.,1989).

The ubiquity of enamel in the teeth of vertebrates from fishes to mammals, its hardness, and its arrangement as a thin outer layer together leave little doubt that its *fundamental* function is to resist abrasive wear. Enamel is anisotropic in its response to abrasive wear (Rensberger and von Koenigswald, 1980) which derives from the fact that apatite crystals abrade less quickly in a direction parallel to the C axis than in a direction normal to the C axis. In the outer enamel, the C axes of the crystallites tend to be directed toward the outer surface, which minimizes the rate of wear in a direction normal to the surface.

The major structural limitation of materials with ceramic-like properties is their brittleness (Clegg, et al., 1990). The brittleness of enamel makes it subject to cracking and thus to initiating failure of the tooth. The tendency to crack limits the degree of stress concentration that can be developed in teeth, which in turn limits the toughness and hardness of food materials that can be physically reduced to small particles by the masticatory system and the speed with which large volumes can be processed. A conspicuous correlate of the early

Cenozoic diversification of mammals was the increase in body size, which raised the maximum level of stress attainable at the occlusal surface through stress concentrating mechanisms. Correlating with larger body sizes was the presence of a new microstructure that improved the crack resistance of enamel (von Koenigswald, et al., 1987) and allowed higher stresses to be attained before fracture. High stress concentrations resulting in tooth loss occur as an accidental and probably frequent event in lower vertebrates, but the evolutionary solution of more rapid tooth replacement was not available to diphyodont mammals, in which the masticatory system is based on precise occlusion (Hopson & Crompton, 1969; Crompton & Sun, 1985).

Thus, owing to high stresses developed in their teeth and the diphyodont tooth replacement scheme, enamel in Cenozoic mammals of medium to large size must have been subject to selection for both crack resistance and abrasion resistance. Fracturing is still a limiting factor in modern Carnivora that heavily load their teeth in the course of eating bones (Van Valkenburgh & Ruff, 1987; Van Valkenburgh, 1988).

Because both enamel and dentin are denser than other hard tissues, teeth are the best preserved structures in the mammalian fossil record. Because of this large resource and its potential information about dietary behaviors, a number of workers have attempted to interpret fossil diets by investigating the relationships between striae, pits, and other features of abrasive wear preserved on both fossil and modern tooth enamel (Teaford, 1988, reviews this literature). As our understanding of how food and teeth interact in processing food (Lucas & Luke, 1984; Janis & Fortelius, 1988), how enamel microstructure influences wear patterns (Maas, 1991), and how enamel microstructural differences are related to differences in the occlusal mechanics of teeth becomes more complete, our ability to utilize this large potential source of information about the evolution of feeding behaviors will proportionately improve.

One of the most widespread types of mammalian enamel consists of Hunter-Schreger bands (HSB), which are layers of alternately directed prisms. This was the enamel type that appeared in at least a few mammals in the early Paleocene and initiated the special strengthening of enamel that accompanied the mammalian diversification (von Koenigswald et al., 1987). Prisms fracture less easily perpendicular than parallel to the long prism axes (Boyde, 1976 ; Rasmussen et al., 1976) and the strength enamel gains through reinforcement by HSB derives from the way crack paths are forced to change direction by decussating prism directions (Pfretzschner, 1988).

The primitive condition for the HSB is one in which the planes between the layers of alternating prism directions are more or less horizontal, as viewed tangentially. At the other extreme of HSB attitude is the structure in rhinocerotoids, in which a 90° rotation of the Hunter-Schreger planes has occurred and the HSB and decussation planes are vertical. In vertical decussation, the adjacent groups of prisms intercept a transverse (horizontal) plane at different angles. In horizontal decussation, the adjacent groups of decussating prisms are nearly parallel to a transverse plane but intercept a radial (vertical) plane at different angles.

Fortelius (1985: Figs. 12, 38, 39) reported vertical decussation in the cheek tooth enamel of *Astrapotherium* sp., a Miocene member of the Astrapotheria, a group of large mammals that were confined to South America until their extinction late in the Cenozoic. Because vertical Hunter-Schreger bands are rare in mammals, and this condition almost certainly arose independently in the two lineages, the degree of similarity of the structure in astrapotheres to that of rhinocerotoids is of particular functional interest because any similarities must have resulted from similar selective pressures rather than from a shared ancestry. In this study we compare the enamel microstructure of astrapothere cheek teeth with that in the rhinocerotoids, describe the microstructure in astrapothere canine enamel, which differs from that in the cheek teeth, and consider the functional implications of these conditions for tooth use.

Institutional Abbreviations

FMNH: Field Museum of Natural History, Chicago, Illinois.
GPIBO: Institut für Paläontologie der Universität, Bonn, Germany
UCMP: University of California Museum of Paleontology, Berkeley, California.
UWBM: Burke Memorial Washington State Museum, University of Washington, Seattle, Washington

Methods

The scanning electron microscope (SEM) examinations of astrapothere enamel microstructure are based on tooth fragments of *Parastrapotherium* (Deseadan, early Oligocene of Pico Truncado, Santa Cruz, Argentina), *Astrapotherium sensu lato* (Friasian, late Miocene La Venta Fauna, Colombia, S.A.), and *Astrapotherium* sp. (Santacrucian, early Miocene, Argentina) that are too incomplete to provide traditional quantitative data about gross tooth morphology and systematic relationships. Similar fragments of *Subhyracodon* (Chadron Formation, early Oligocene, South Dakota), a rhinocerotoid, were examined for comparison, along with published descriptions of rhinocerotoid enamel. For the canine enamel structure, we removed an inconsequential fragment from the margin of an existing fracture in the canine of two taxa. Each prepared enamel fragment is identified by a suffix added to the original museum catalogue number and is being returned to the original museum collection along with a description of the position and orientation of the fragment on the tooth.

Sections of enamel were examined in three planes (Fig. 1): tangential (parallel to the outer surface), radial (parallel to the long axis of the tooth and normal to the outer surface) and transverse (normal to the long axis of the tooth). Figured tangential and radial sections are oriented with the occlusal direction toward the top of the figure unless otherwise indicated by a hollow arrow.

Because of the anisotropic behavior of enamel to fracturing as well as to corrosion by acid, the microstructure is visible in either broken surfaces or polished and acid-etched surfaces. All of the astrapothere teeth in the FMNH and UCMP collections were examined under low power light microscopy. Most of the transverse and radial sections of enamel fragments were first examined as broken, unpolished and unetched surfaces with the SEM. The relief of broken sections gives an indication of the resistance of the microstructure to fracturing and allows recording structural differences at low SEM magnifications of large areas of enamel. These sections were subsequently examined as

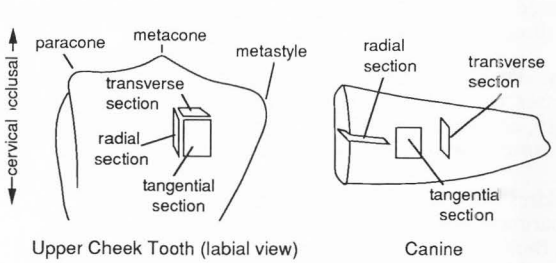

Figure 1. Orientation of sections.

polished sections etched in dilute hydrochloric acid for 5 to 15 seconds. The polished sections were either initially ground using coarse (150 or 360) grit silicon carbide wet-dry paper followed by finer paper through 1200 grit, or ground with a silicon carbide stone followed by polishing with a wet slurry of silicon carbide powder. For tangential sections, the outer enamel was removed into the zone of vertical decussation, which varies in depth, either by air abrasion with dry aluminum oxide powder or by grinding.

A theoretical prediction of the loading directions of the canine in life was obtained by calculating the principal stresses for a finite element model, using the microcomputer application MSC/pal2, and comparing the cracks predicted by the model to those observed in the canine enamel.

Empirical data for stress directions were found by identifying premortem cracks in the enamel. Cracks were recognized as premortem when their edges bear a polish resulting from chewing or other usage of the teeth (Rensberger, 1987). The evidence that such abrasion is due to premortem activities and not to postmortem depositional processes is the differential distribution of the polish, especially its confinement near the occlusal surface of the cheek teeth or near the tip of the canine.

Crack directions in the canines were measured by photographing and digitizing the cracks and analyzing the directions with a microcomputer application, Macazimuth. This application, in effect, repeatedly steps one pixel at a time along the graphic line representing a crack and measures the direction of a point on the line at a specified distance ahead. As the algorithm proceeds, the part of the line covered is recorded separately so that no lines are retraced as a result of crack junctions. The program is written in FORTH and runs on a Macintosh computer.

In this study, each azimuth is the angle in a plane tangent to the enamel surface measured clockwise from the lingual direction to the crack direction (the direction parallel to the longitudinal or cervical-occlusal axis of the tooth would be 90°. The direction of the crack is based on the direction formed by a line connecting a given pixel on the crack with the next pixel whose x or y coordinate is exactly 6 pixels distant. This allows discrimination of 24 directions, an increase in precision compared to a similar algorithm used by Rensberger, Forstén and Fortelius (1984). In the latter algorithm, each azimuth was based on the second closest pixel ahead, yielding 8 possible directions. For additional details about the method, see Rensberger, et al. (1984).

The 24 azimuths discriminated by 6 pixel separation are: 0°, 9.5°, 18.4°, 26.6°, 33.7°, 39.8°, 45°, 50.2°, 56.3°, 63.4°, 71.6°, 80.5°, 90°, 99.5°, 108.4°, 116.6°, 123.7°, 129.8°, 135°, 140.2°, 146.3°, 153.4°, 161.6°, and 170.5°.

A tradeoff of the 24 azimuth algorithm is the greater tendency to average away small bends in the structure being measured. This is a useful constraint here because the objective is to document differences in the directions in which stresses acted in causing the cracks; fine irregularities in crack paths are expected to be the result of material properties rather than stress directions.

A correction is applied to the raw frequencies to make all azimuths equally probable. In a digital image, a line connecting two diagonal pixels is longer than one connecting two pixels along the x or y axes. Without correction, unequal frequencies of azimuths would be sampled along cracks of equal length running in different directions.

Astrapothere Molar Enamel

The following descriptions are based on reflected light microscopic and SEM examinations of molar enamel sections and surfaces in *Astrapotherium* from middle and earlier Miocene, and reflected light microscopic examination of molar enamel sections and surfaces in *Parastrapotherium*.

Vertical decussation

Sets of prisms running in different directions are most clearly defined in sections normal to the decussation plane. In the case of vertical decussation, transverse and tangential sections offer good zone delineation. The structure in each of these views is discussed below.

In transverse sections of molar enamel in astrapotheres (Fig. 2), the alternating HSB are as prominent and uniformly defined as in rhinocerotoids. The prisms of one of these zones correspond in structure to the set labelled B in rhinocerotoids by Rensberger and von Koenigswald (1980) and begin growing in an obliquely outward and cervical direction from the enamel-dentin junction (EDJ). Then, as the zone narrows slightly near the middle of the enamel thickness, the prisms of this set become horizontal (Fig. 3). The prisms of the adjacent set on either side (corresponding to set A in rhinocerotoids) run occlusally and outward. This set transversely widens slightly in the middle of the enamel and appears to continue with little change toward the outer edge (Fig. 2). Higher magnification is needed to show the reversed directions of the prisms of sets A and B (Fig. 4). Sets A and B are separated by a thin band of transitional prisms of almost horizontal attitude (Fig. 4).

In radial sections of astrapothere enamel, the inner enamel shows the strong angular divergence of prisms sets A and B (Fig. 5) that characterizes rhinocerotoid enamel (Rensberger and von Koenigswald, 1980, Figs. 7, 8). In the outer part of the enamel the distinctiveness of these zones disappears and all prisms are outwardly and upwardly directed (Fig. 5). To achieve this occlusal-outward slant, the prisms with an initial cervical-outward direction (set B) bend abruptly in the middle region of the enamel (Fig. 6).

The astrapotheres strongly resemble the rhinocerotoids in all these details (Rensberger and von Koenigswald, 1980, Figs. 3, 4, 5, 7, 8); Boyde and Fortelius, 1986, Figs. 20, 21-23).

As a consequence of the combination of sharply differentiated zones of vertically decussating prisms and the equally distinct thin zone of transitional prisms with horizontal attitude, the more or less horizontal occlusal surfaces of molar enamel bear a ridge and valley relief (Fortelius, 1985, Fig. 38) like that in rhinocerotoids (Rensberger and von Koenigswald, 1980, Fig. 2; Fortelius, 1985, Figs. 18, 32, 38). The relief is caused by the dependence of wear resistance of hydroxyapatite crystals upon their alignment and the tendency for the average direction of crystallites making up a prism to be parallel to the long axis of the prism.

In a tangential section (Fig. 7), the HSB are highly uniform in width and sharply defined. The uniformity of width is maintained through the occasional fission or termination of a band. The prisms of the darker bands are those of set B (descending from the EDJ) and those of the lighter bands are of set A (ascending). The transitional zone (containing prisms normal to the section) between adjacent HSB is narrow and uniform in width (Fig. 8). The similarity in this view to the structure in rhinocerotoids (Figs. 9, 10; Boyde and Fortelius, 1986, Fig. 10) is as strong as that noted for the transverse section.

Horizontal decussation

In the outer enamel, in which the prisms of set B generally run in an outward and slightly inclined direction toward the occlusal surface, a second zone of decussation exists. In polished radial sections, rather regularly spaced bands can be seen within the outer enamel (Fig. 11). The long axes of these narrow bands run outward and slant somewhat toward occlusal surface, in parallel with the general prism direction of the outer enamel. At higher magnification (Fig. 12) the constituent prisms of these bands can be seen to

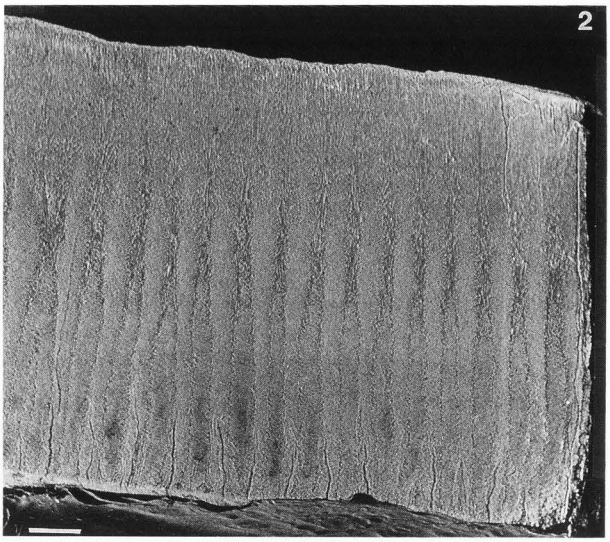

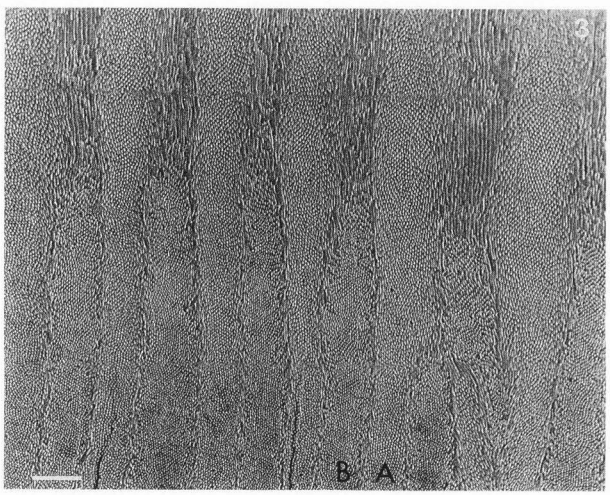

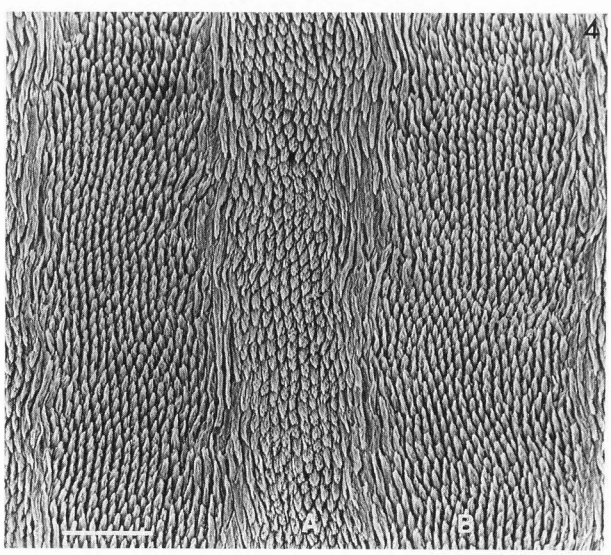

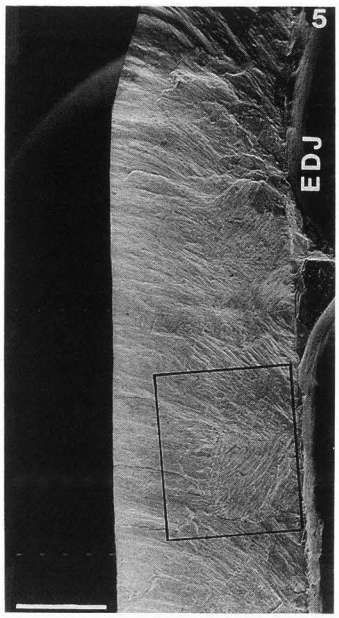

Figure 5. *Astrapotherium s. l.*, UCMP 38825BLT, fractured, unground, unetched radial (vertical) section of lower molar enamel. EDJ at right, occlusal toward top (beveled left upper margin is wear facet). Vertical decussation confined to approximately inner half of enamel thickness. Bar = 1 mm.

Figure 2. *Astrapotherium sensu lato*, UCMP 38825B. This and subsequent UCMP specimens from La Venta Fauna, Colombia, S. A. (Friasian, late Miocene). This taxon is being described and assigned to a new genus by Steve Johnson and Rick Madden (Johnson, pers. comm.). Transverse polished and acid-etched straight section of lower molar enamel, viewed from cervical to occlusal. EDJ at bottom, outer surface at top. Bar = 200 μm.

Figure 3. *Astrapotherium s. l.*, UCMP 38825B, orientation as in Fig. 2 but enlarged, showing well-defined boundaries of decussation zones in central region. A, zone with prisms running occlusally and outward; B, zone with prisms running cervically and outward (see Fig. 4). Prisms of zone B bend and become horizontal near upper part of micrograph while prisms of zone A continue in their occlusally directed course. Bar = 100 μm.

Figure 4. *Astrapotherium s. l.*, UCMP 38825B, central region of Fig. 3 enlarged, showing reversed prism directions in zones A and B, horizontal attitude of prisms in transitional zones. Bar = 50 μm.

intercept the radial plane at a different angle than the prisms of the surrounding enamel. These prisms therefore have the same relationship to the vertical plane as horizontal HSB, that is, the plane of decussation is normal to the vertical plane. These zones of horizontal decussation are not to be confused with the faint continuation of vertical decussation that is sometimes present in the outer enamel of rhinocerotoids (Boyde and Fortelius, 1986).

The angle of decussation (angle between crossing prisms) in the horizontal HSB (Fig. 12), is usually less than the angle of vertically decussating prisms in the inner enamel, and the zones occupy a smaller interval of the enamel thickness. The borders of the zones are usually less well-defined than those of the vertically decussating inner enamel, but in one specimen we examined the decussation is strong and the zones are well-defined and are separated by a thin zone of transitional prisms (Figs. 13, 14). The zones of horizontal HSB in the outer enamel represent a tissue distinct and unrelated to the vertically decussating zones of the inner enamel. An interval in which there is no decussation usually separates the two (Fig. 12).

Previous studies found only vertical prism decussation in

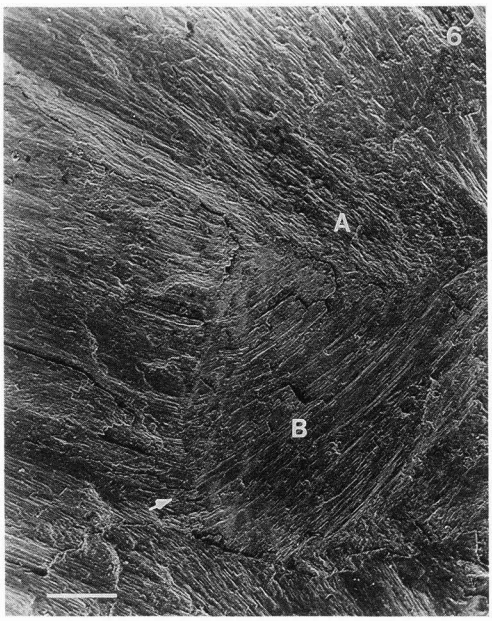

Figure 6. *Astrapotherium s. l.*, UCMP 38825BLT, region of box in Fig. 5, fractured unground section showing cervically running zone B prisms (near center, below zone A prisms) turning upward at boundary between the inner and outer enamel (arrow). Note relatively smooth vertical fracture surface across both zones. Bar = 200 µm.

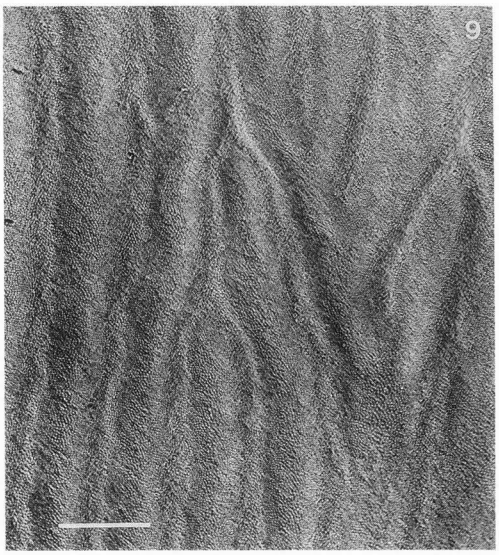

Figure 7. *Astrapotherium s. l.*, UCMP 38063BM, tangential ground section of lower molar enamel, viewed toward EDJ, occlusal direction toward top. Outermost enamel removed to expose zones of vertically decussating prisms. Prisms in dark tracts cervically directed (zone B). Bar = 200 µm.

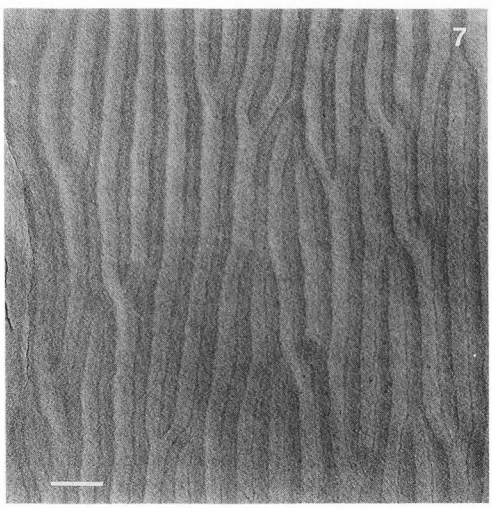

Figure 8. *Astrapotherium s. l.*, UCMP 38063BM, tangential section, as in Fig. 7 but at higher magnification, showing horizontal prisms of transitional zone (normal to plane of section) bounding occlusally and cervically running prisms of zones A and B. Bar = 100 µm.

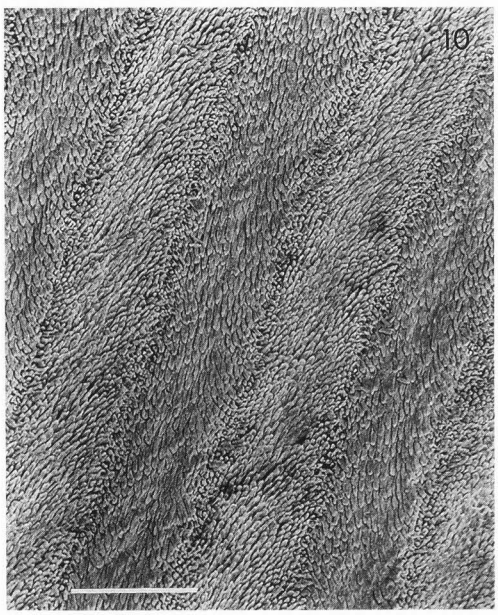

Figure 9. *Subhyracodon*, UWBM 32019, a rhinocerotid, early Oligocene, N. A. Tangential section of ectoloph inner enamel of upper molar, viewed toward EDJ, occlusal toward top. Relief caused by variation in resistance of enamel to air abrasion jet depending on prism direction. Bar = 200 µm.

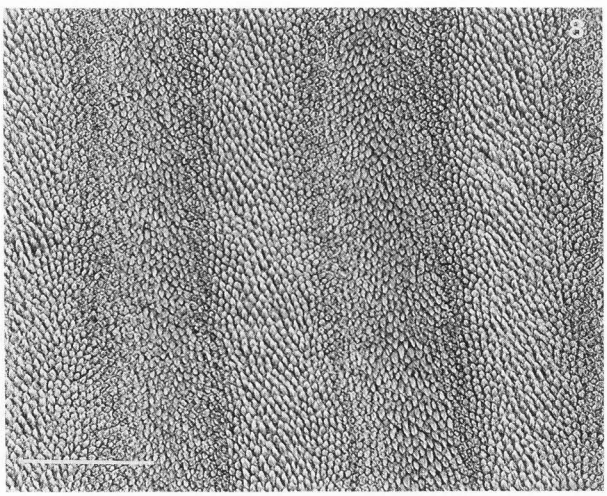

Figure 10. *Subhyracodon*, UWBM 32019, tangential section of inner enamel of upper molar ectoloph, showing horizontal prisms of transitional zone and occlusally and cervically running prisms of zones A and B. Bar = 100 µm.

the cheek tooth enamel of rhinocerotoids (Rensberger and von Koenigswald, 1980; Fortelius, 1985; Boyde and Fortelius, 1986). However, horizontal decussation occurs in the outer enamel of rhinocerotoids; the condition there and its relationship to that in astrapotheres will be described in a separate study.

Astrapothere Canine Enamel

Canine tusk enlargement is characteristic of astrapotheres and goes back to the most primitive known genus, the early Eocene *Trigonostylops* (Cifelli, 1983b). The structure in the canine is distinct from that in the cheek teeth. The following descriptions are based mainly on SEM examination of sections

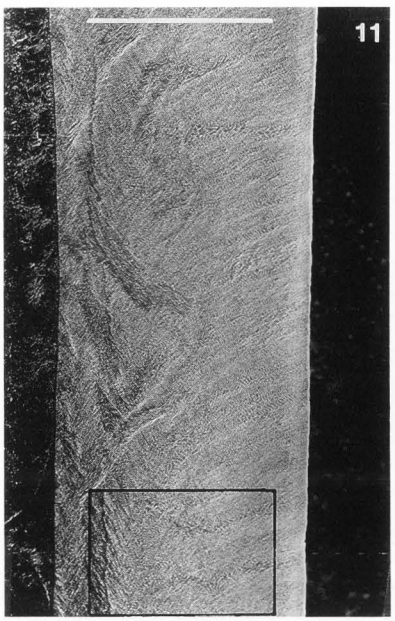

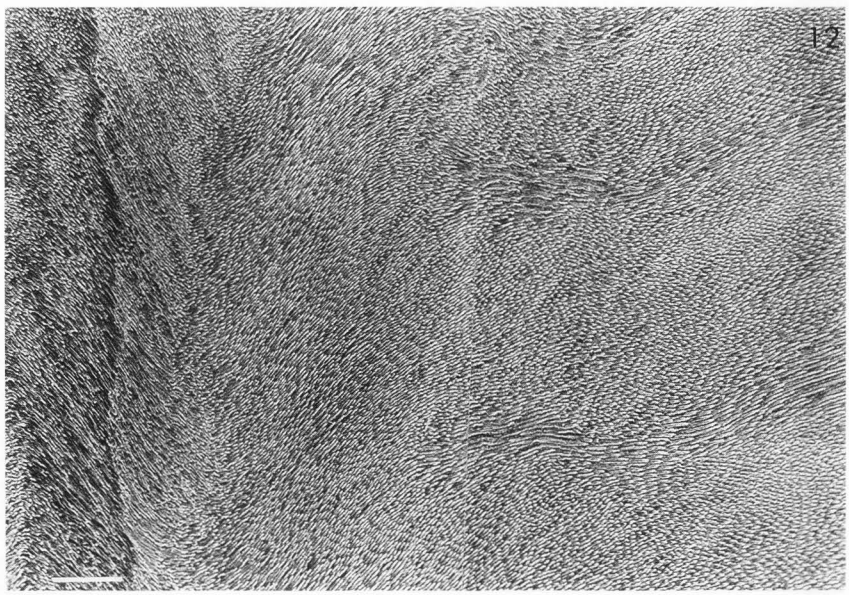

Figure 11. *Astrapotherium s. l.*, UCMP 38825AY, polished and etched radial section of lower molar enamel showing vertical prism decussation in inner half of enamel thickness and banded pattern in outer enamel. EDJ at left. Section occurs in region of strong horizontal curvature of enamel plate. Bar = 1 mm.

Figure 12. *Astrapotherium s. l.*, UCMP 38825AY, region of box in Fig. 11, showing horizontally decussating prism zones in outer enamel. Bar = 100 μm.

because the complexity of the structure limits the interpretation of unsectioned specimens examined under reflected light.

Parastrapotherium

The enamel structure in the canines of the astrapotheres examined is quite distinct from that in the molars. In tangential view of a lower canine of *Parastrapotherium* in which the outer enamel has been removed (Fig. 15), sets of prisms running in different directions form zig-zag bands, resembling a series of waves. These bands run occlusally, i.e., longitudinally toward the tip of the tooth (toward the top of the micrograph in this figure). The crests and troughs in these arcuate bands are aligned obliquely transverse (slanting slightly downward in the micrograph, left to right). This structure appears in tangential view to represent vertical HSB because the bands tend to be continuous in the occlusal direction (Fig. 16), but the transverse alignment of the sinusoidal crests and troughs gives the appearance of horizontal HSB. The angle of decussation of the prisms in adjacent bands in the tangential section of Figures 15 and 16 is often about 45°, but may be as much as 80°, as can be seen along the margin of the crack in Figure 17.

The directions of the prisms of the inner part of the canine enamel in radial section (Fig. 18) resemble those in the vertically decussating part of the molar enamel. The prisms run more or less within the vertical plane in two directions that differ by 70° to 80°. One set slants cervically from the EDJ and the other occlusally.

In transverse section (Fig. 19), the structure near the EDJ (right side of the micrograph) contains transversely elongated zones of prisms intercepting the plane of the section at a high angle, separated by a zone of prisms running parallel with the plane of the section. The prism direction in each adjacent zone of high angle prisms is the reverse of the

Figure 13. *Astrapotherium* sp., GPIBO, Santacrucian (early Miocene, Argentina), radial section through lingual margin of upper molar protocone in center of outer enamel, occlusal direction toward top, outer surface toward left. Well-defined horizontal decussation with narrow transitional zones. Bar = 100 μm.

Figure 14. *Astrapotherium* sp., same specimen, section, and orientation as Fig. 13, but to right of that frame, showing junction of inner and outer enamel. EDJ off frame at right. Cervically running prisms of zone B (at right) bend occlusally, begin decussating horizontally. Bar = 100 μm.

Figure 15. *Parastrapotherium*, FMNH P15050LT1, Pico Truncado, Santa Cruz, Argentina (Deseadan, early Oligocene), tangential section of lower canine enamel, direction of tip toward top, viewed toward EDJ. Showing aligned arcuate bands of differently directed prisms and sinuous paths of cracks. Bands aligned longitudinally, wave crests aligned transversely. Outermost enamel removed by air abrasion. Image contrast results from differential "specimen collection" of electrons (Borchert, Vecchi, & Stein, 1991), here a blockage of secondary electrons produced in depressions related to different prism directions (see Fig. 16). The effect produces a map of prism divergence at magnifications too low to resolve prisms. Bar = 200 μm.

Figure 16. *Parastrapotherium*, FMNH P15050LT1, higher magnification near frame of Fig. 15, showing wavelike changes in prism direction that produce bands in Fig. 15. Bar = 50 μm.

Figure 17. *Parastrapotherium*, FMNH P15050LT1, region of box in Fig. 15, showing relationship of prism directions in crack walls to crack directions. Along crack, local change in prism direction is associated with positions of knoblike bends in crack wall. Bar = 50 μm.

Figure 18. *Parastrapotherium*, FMNH P15050LT3, polished and etched radial section of inner part of lower canine enamel, EDJ at left; showing aspects of both horizontal and vertical decussation. Inner enamel with prisms dominantly parallel to vertical plane of section, some running outward and cervically (zone B prisms), others running outward and occlusally, as in vertical decussation. However, some prisms of inner enamel turning horizontally to intercept plane of section at high angle (e.g., near bottom of frame), as in horizontal decussation.
Bar = 100 μm.

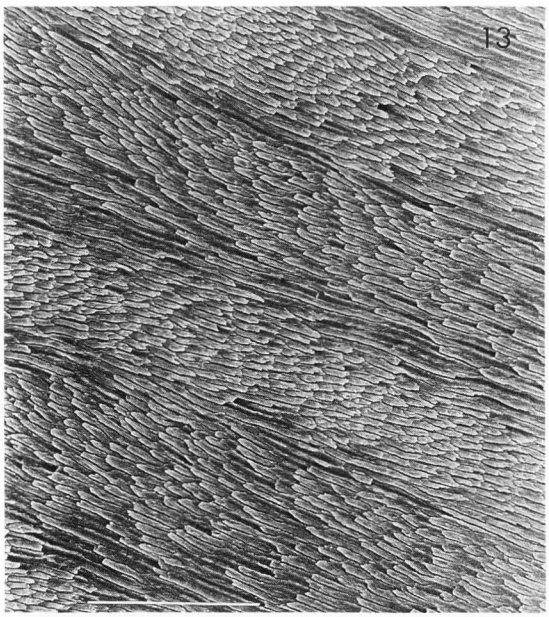
13

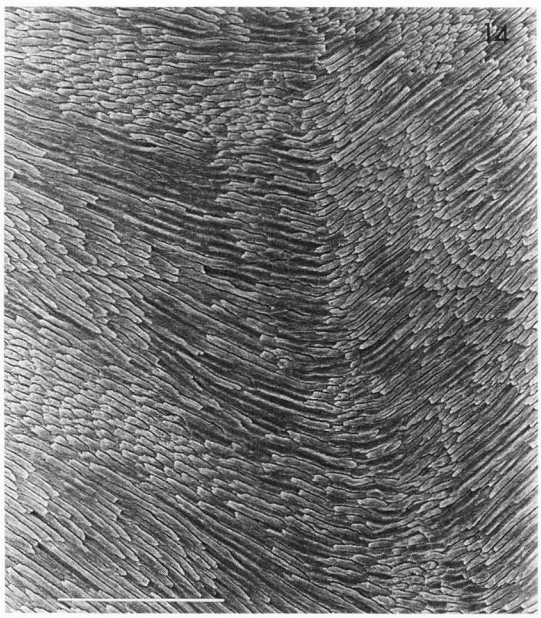
14

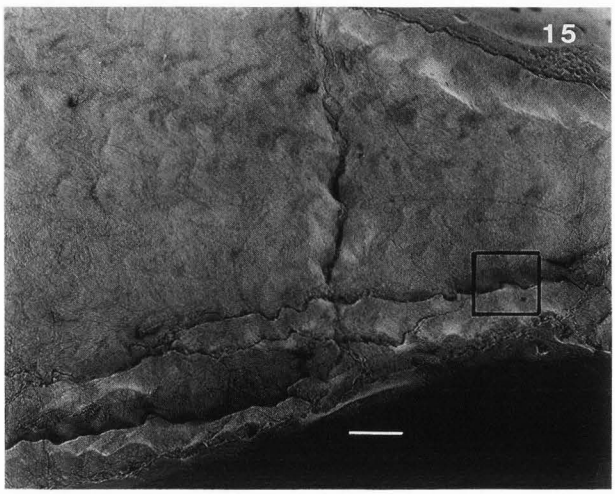
15

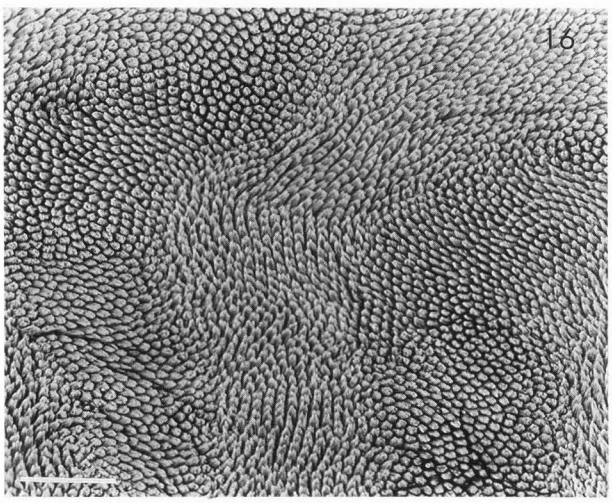
16

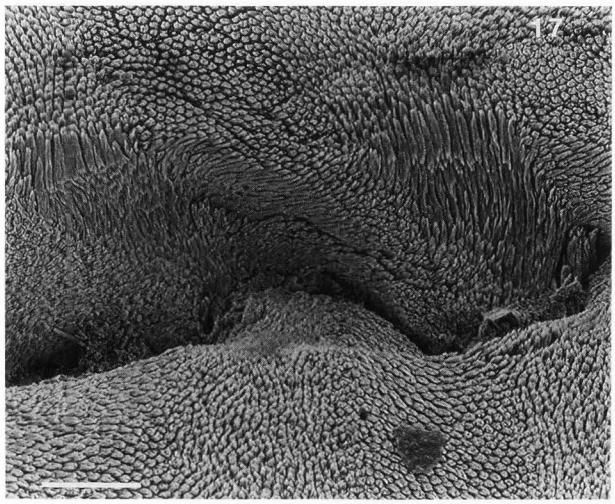
17

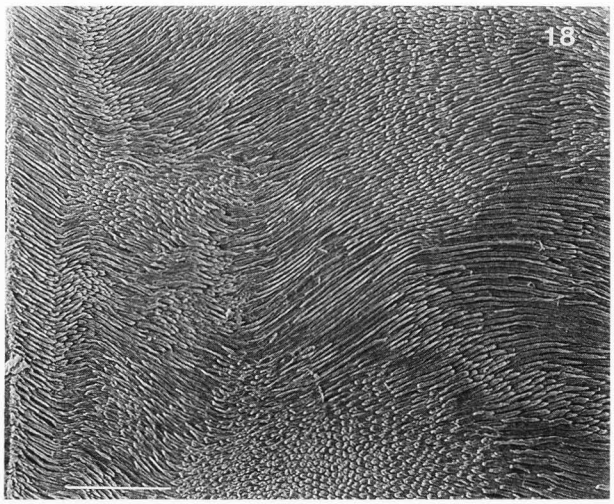
18

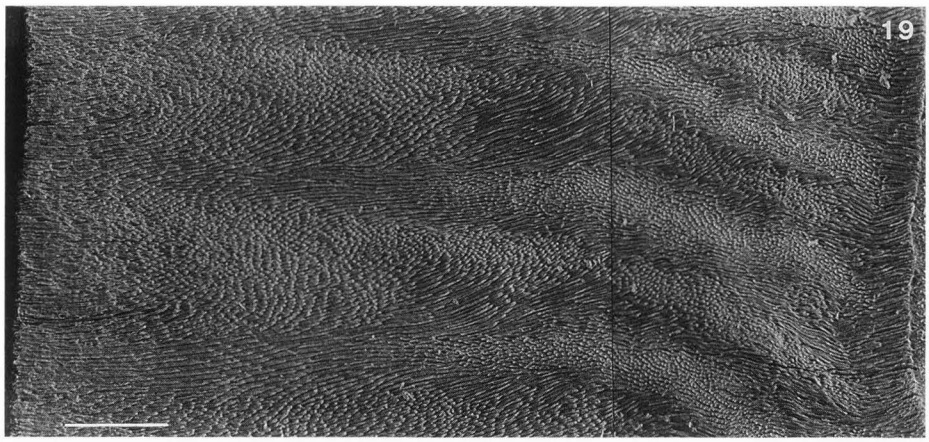
19

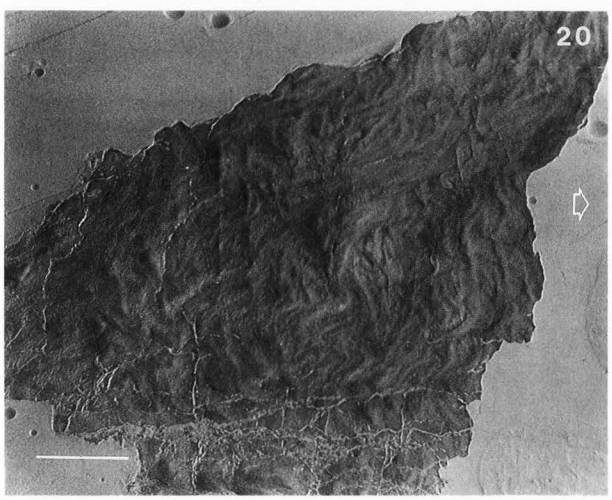
20

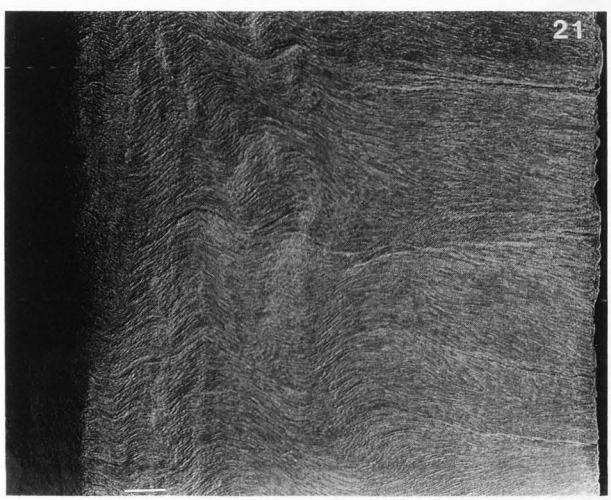
21

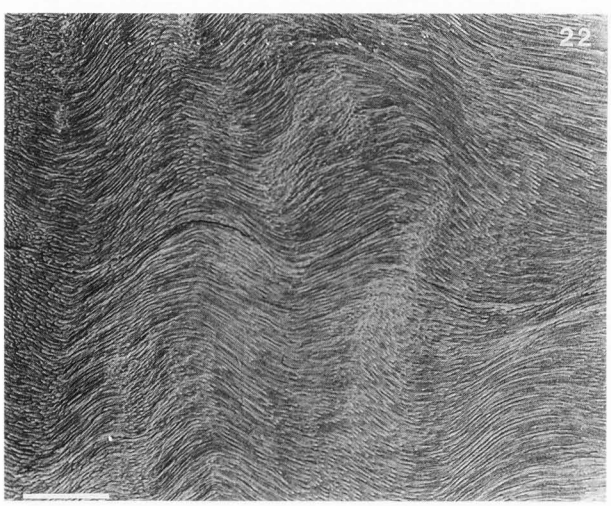
22

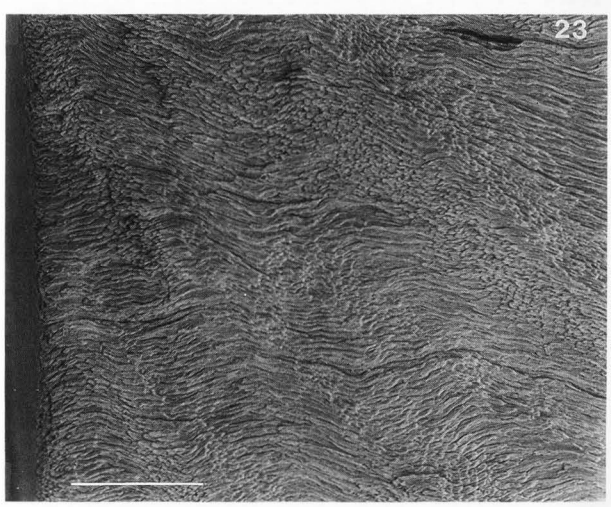
23

Figure 19. *Parastrapotherium*, FMNH P15050LT3, polished and etched transverse section of lower canine enamel, from EDJ at right to outer surface at left; vertical decussation in inner enamel similar to that in molars, but zones bending within transverse plane and obliquely transverse in direction. In outer enamel zones become transverse. In central region there is some divergence of prism direction within horizontal plane, that is, some degree of horizontal decussation, but unlike that in molars. Decussation extends through greater part of enamel thickness than in molars. Bar = 100 μm.

Figure 20. *Astrapotherium s. l.*, UCMP 29230AC, tangential section of polished and etched upper canine enamel fragment, occlusal direction toward right (arrow). Outer enamel removed. Gentle variation in direction of prisms emerging on etched surface causes apparent "ridges" whose pattern reflects the differences in prism direction. Bar = 1 mm.

Figure 21. *Astrapotherium s. l.*, UCMP 29230AO, air abraded, etched transverse section of upper canine enamel, viewed occlusally, showing wavelike bending of prisms that diminishes in outer enamel. EDJ at left. Bar = 100 μm.

Figure 22. *Astrapotherium s. l.*, UCMP 29230AO, enlargement of central region of Fig. 21. Bar = 100 μm.

Figure 23. *Astrapotherium s. l.*, UCMP 29230AO, air abraded, etched radial section of upper canine enamel, occlusal direction toward top, EDJ at left. Wavelike bending of prisms, axes of bends running cervically and outward (from upper left to lower right). Because some prism bending occurs in horizontal planes, ground section transects prism axes along certain sides of folds. Bar = 100 μm.

direction in the neighboring high angle zone, with the prisms of one slanting toward the EDJ and those of the other slanting toward the outer surface. The structure resembles that in the molar enamel because in both cases vertically decussating sets of high angle prisms are separated by zones of prisms parallel with the transverse section.

The structure of the canine enamel in transverse section differs from that in the molars in several ways, however. The HSB in the canines extend obliquely from the EDJ but bend and become perpendicular to the latter toward the middle of the enamel thickness, whereas in the molars the zones are perpendicular to the EDJ throughout their extent. The prisms that rise (run occlusally) from the EDJ in the canine become horizontal near the middle of the enamel, whereas those that run cervically from the EDJ flatten their trajectory somewhat but continue toward the outer surface in a slightly cervical direction.

In summary, the lower canine enamel of *Parastrapotherium*, like the molar enamel in all of the astrapotheres we have seen, is dominated by a pattern of vertical decussation. However, as seen in transverse section, the HSB of the inner enamel are aligned oblique to the EDJ and are curved, rather than perpendicular and straight. In tangential section, the HSB have more or less regular wavelike bends whose crests are aligned in the vertical (occlusal) and horizontal (transverse) directions so that they appear to combine aspects of vertical and horizontal decussation.

La Venta Astrapothere

Although upper canine enamel from *Parastrapotherium* was not seen in this study, we examined enamel in the upper canine of a late Miocene form, *Astrapotherium s. l.* from the La Venta fauna of Colombia.

In tangential section, the La Venta astrapothere lacks the regular wavelike bending of differently oriented groups of prisms present in *Parastrapotherium*. The different prism directions beneath the featureless region of the outer enamel have an overall pattern that is much more random (Fig. 20) than that in *Parastrapotherium*. The bands of similarly directed prisms in some areas run cervical to occlusal (e.g., above center of figure) but in much of the fragment they tend to be more transversely aligned. Parallel sinuous bends, as seen below the center of the fragment, are similar to the pattern in *Parastrapotherium*, but overall the structure in tangential section lacks the regularity of the Oligocene form.

In transverse section (Fig. 21), it can be seen that the prisms form a wavy pattern in which the prisms of adjacent bands tend to parallel one another rather than decussate. The bending occurs mainly within the transverse plane (Fig. 22), although there is some vertical bending. The axes of the waves themselves bend and may be aligned in different directions (e.g., the slanting alignment of the wave left of center in the upper part of Figure 21).

In ground radial section (Fig. 23), the prisms in the La Venta form appear to form parallel waves whose axes trend obliquely in the cervical direction from the EDJ. In a ground section it is difficult to distinguish between simple bending of prisms and decussation. In a fractured, unground radial section (Fig. 24), oblique ridges represent the same cervically trending waves seen in Figure 23. In Figure 25 the shadowed upper third of the image represents the same radial (vertical) fracture surface shown in Figure 24; the lower two-thirds of the image is a transverse (horizontal) surface adjoining the radial surface. The undulating border (outer end marked by arrow) between these horizontal and vertical surfaces is paralleled by prisms near the edge bending in the horizontal plane. These undulations form the prominent ridges on the vertical surface, indicating that the enamel structure consists mainly of bending prisms, not decussation.

Von Koenigswald (1988:150), reported transverse HSB in an upper canine (astrapothere, gen. & sp. indeterminate). The structure he saw under light microscopy (pers. comm.) may be similar to that in the La Venta form. Under light the structure in the La Venta form appears to represent horizontal HSB.

Functional Interpretation

Molar Enamel

In theory, horizontal HSB optimally resist the propagation of vertical cracks; in the primitive ungulates that have rounded cusps and dominantly vertical chewing movements (e.g. *Arctocyon* and other condylarths, and *Hyracotherium*), the maximum stresses are expected to be horizontal and tensile. This has been demonstrated by both mathematical and physical models (Fig. 26; Pfretzschner, 1988; Rensberger, in press). However for later, large ungulates, finite element modelling demonstrates several ways in which stresses may change (Pfretzschner, in press a, b; Rensberger, in press). In rhinocerotoid cheek teeth, the direction of maximum stress is vertical, judging from the directions of premortem cracks as well as results of finite element modelling of the principal stresses. The explanation for this 90° rotation of the principal stresses is that the occlusal structures have become thin lophs and the chewing force has become dominantly perpendicular to the plane of the loph, causing the structure to bend along a horizontal axis (Fig. 26). The planes of decussation of the HSB, which are more or less horizontal in primitive ungulates, have also rotated 90° in rhinocerotoids, and this allows the enamel to maximally resist cracking under the new stress regime.

The molars of astrapotheres, especially the uppers, strongly resemble those of rhinocerotoids (Fig. 27). In both groups the labial part of the upper molar forms a thin, vertical, bladelike ectoloph. Although the ectoloph is blunted by wear in the illustrated individuals, the plane of wear slopes linguad and actually maintains an acute labial edge. In both groups the labial surface of the ectoloph is almost flat, marked only by a narrow, vertical paracone fold and by a slight convexity near

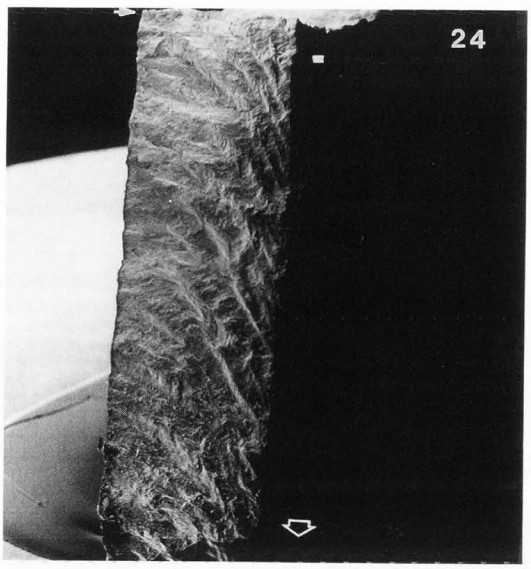
24

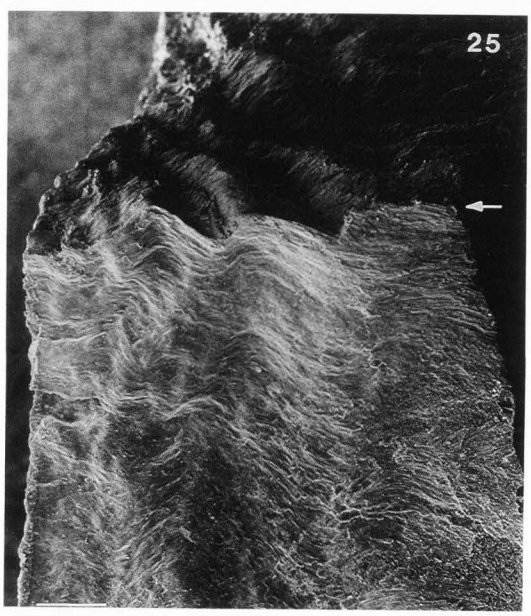
25

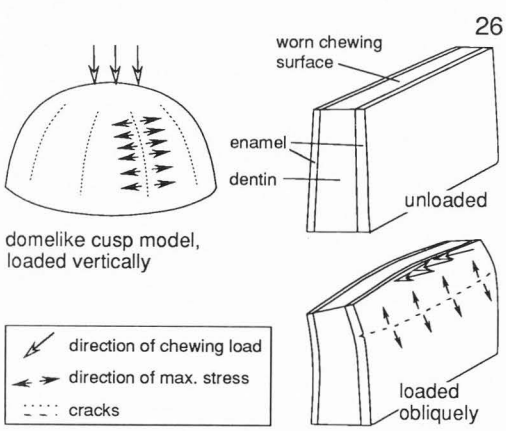
26
worn chewing surface
enamel
dentin
unloaded
loaded obliquely
domelike cusp model, loaded vertically
direction of chewing load
direction of max. stress
cracks

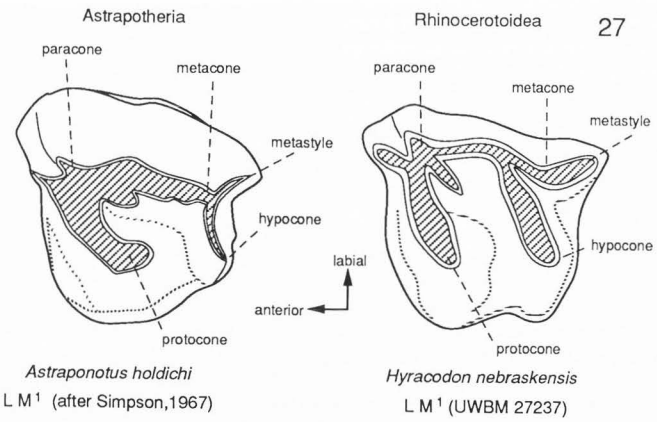
Astrapotheria
Rhinocerotoidea
27
paracone
metacone
metastyle
hypocone
labial
anterior
protocone
Astraponotus holdichi
L M1 (after Simpson,1967)
Hyracodon nebraskensis
L M1 (UWBM 27237)

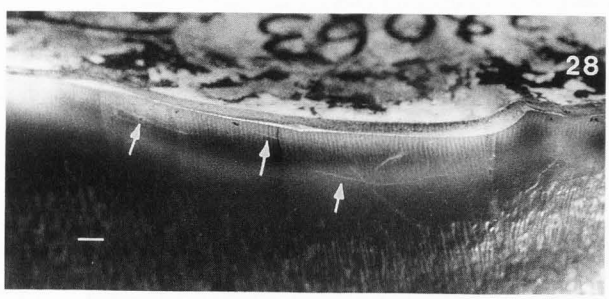
28

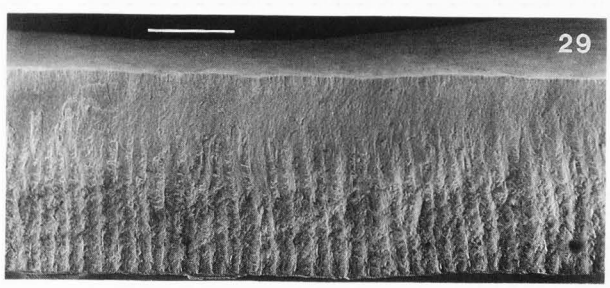
29

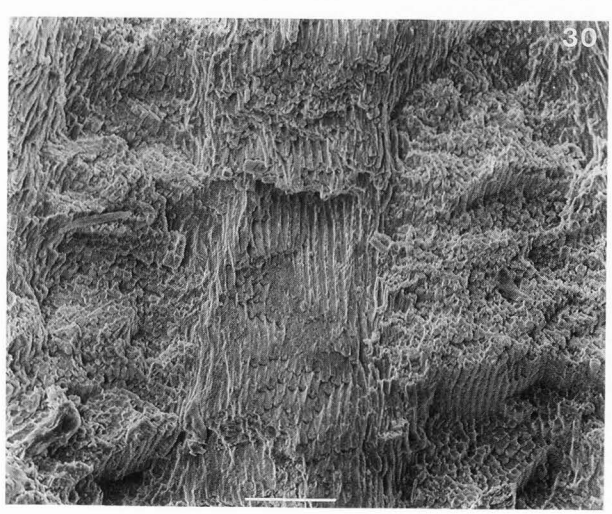
30

Figure 24. *Astrapotherium s. l.*, UCMP 29230AO, upper canine enamel, unground, unetched radial fracture with rugose surface (surface of Fig. 23 before air abrading). Occlusal direction toward bottom, EDJ at right edge. Arrow indicates outer corner marked in Fig. 25. Bar = 100 μm.

Figure 25. *Astrapotherium s. l.*, UCMP 23230AO, upper canine enamel, unground, unetched transverse fracture surface, top surface of enamel segment in Fig. 24 looking occlusally, with vertical face of Fig. 24 visible as shadowed and ridged face at top of this Figure. Arrow identifies outer corner of edge between transverse and radial sections marked in Fig. 24. EDJ at left edge. Bar = 100 μm.

Figure 26. Effect of extreme differences in shape of dental structure and direction of load on maximum stresses in enamel. Model on left depicts state in shell of stiff material covering less stiff interior, subjected to dominantly vertical load (as in early Cenozoic ungulates). Models at right demonstrate deformation and stresses in narrow loph subjected to oblique load (as in rhinocerotoids and astrapotheres); maximum stress, which is tensile, is rotated 90°.

Figure 27. Occlusal views of upper molar in astrapothere and rhinocerotoid. Shaded areas represent dentin exposed by wear.

Figure 28. *Astrapotherium s. l.* upper molar, UCMP 38063, labial view. Light micrograph showing light reflecting from planes of horizontal premortem cracks (arrows) in ectoloph enamel, near occlusal edge (above arrows). Light colored oblique line crossing crack at right is a surface blemish. Vertical HSB visible near edge of enamel. Dark vertical cracks are postmortem. Bar = 1 mm.

Figure 29. *Astrapotherium s. l.*, UCMP 38825B. Transverse (fractured, unground, unetched) section of lower molar enamel looking occlusally, with extremely rugose fracture surface through inner enamel. EDJ at bottom of figure. Bar = 1 mm.

Figure 30. *Astrapotherium s. l.*, UCMP 38825B, subregion of inner enamel of Fig. 29 at higher magnification, showing fracture surface plunging parallel to decussating prism directions in planes almost perpendicular to one another. Bar = 50 μm.

---

the metacone (see also Fig. 1). In both groups, the interior cusps of the upper molar (protocone and hypocone) are incorporated into narrow, posterolingually slanting lophs.

The premortem cracks present in the astrapothere ectoloph (Fig. 28) are horizontally elongate and shallowly concave toward the occlusal edge of the enamel. These cracks have precisely the shape and orientation of the lenticular premortem cracks that characterize the ectoloph of rhinocerotoids and significantly differ in these characteristics from cracks in the less derived cheek teeth of *Mesohippus* and probably other perissodactyls (Rensberger, in press: Fig. 12).

A transverse fracture through molar enamel in *Astrapotherium* produces an extremely rugose surface across the inner enamel where vertical decussation occurs (Fig. 29). At this magnification the surface seems to consist of ridges and valleys, but at a higher magnification (Fig. 30) the surface is seen to have stepped features in which the fractures parallel groups of prisms into the enamel before breaking across the prism axes. The prisms and prism clusters act as fibers and much of the crack energy is absorbed by the pull-out of these fibers. For fractures in this plane the enamel gains its toughness through a mechanism similar to that of the fabric in the thrust deflector used on the French Mirage jets, in which a high-strength brittle fiber traces the strain lines in a brittle matrix (Besmann, et al., 1991).

The similar microstructures, stresses, and overall occlusal shapes are all derived, not primitive conditions in astrapotheres and rhinocerotoids. Because these taxa were isolated throughout their existences and do not share an ancestor that had these structural conditions, a similar set of selective factors must have been responsible. Strains resulting from vertical tensile stresses must have been dominant during mastication, and occasionally these would be great enough to cause horizontal fracturing of the occlusal enamel and consequent loss of chewing effectiveness in that locus. Vertical HSB seem to have provided an effective reinforcement against those strains. However, in the larger sample of rhinocerotoid teeth examined, several segments of horizontally fractured and subsequently worn enamel edges were found (Rensberger, in press; Figs. 12, 13), indicating that sometimes chewing induced vertical tensile stresses exceeded the strength of the material.

Canine enamel

Premortem cracks are abundant near the tip of the lower canine of *Parastrapotherium* (Figs. 31, 32). In this area the enamel has a smoothly worn surface formed by abrasive contact with food or other environmental materials. Only a few of the cracks exposed at the surface do not have edges rounded by such abrasion.

The frequency distribution of the premortem crack directions on the labial enamel plate (Fig. 33) has prominent modes at 146.3° to 153.4° and at 71.6°, indicating at least two rather different sets of crack directions and stress regimes.

After calculating the premortem crack frequencies for the lingual enamel of the same tooth, it became apparent that the dominant crack directions are similar to those near the dominant modal value (146°) in the labial enamel, but the distribution lacks the 71.6° mode exhibited by the labial cracks. Other cracks exist in the lingual enamel that initially had been excluded because they do not reach the surface and could not be differentiated on the basis of wear from cracks formed by postmortem events. When the azimuths of the undifferentiated lingual cracks are added to those of the premortem cracks the 146.3° mode is not appreciably affected (Fig. 34), but the resemblance to the labial crack directions is strengthened by the addition of azimuths near the missing 71.6° mode. It therefore appears likely that the deeper cracks in the lingual enamel were also formed by premortem events and the crack systems on the two sides are the result of transverse and obliquely longitudinal stress regimes. The cracks on the lingual side tend to bend more strongly; the transverse cracks slant in a more longitudinal direction toward the bottom of Figure 35B, producing a 123.7° mode adjacent to the 146.3° mode; bending of the longitudinal cracks spreads their range of direction and flattens that mode. If the longitudinal cracks on the lingual side (those from 39.8° to 71.6°) were due to bending from a labial load, the deeper part of the enamel on the lingual side would have greater tensile stress than the outer part, resulting in deep cracks like those observed that do not reach the surface.

The plane of the cracks in both labial and lingual enamel that reach the outer surface tend to dip away from the tip of the canine. The cracks of the major modal direction (146.3°) on the labial enamel plate are reproducible by a load (L1) near the tip of the tooth, normal to the surface, and above the longitudinal axis (Fig. 35A). The enamel is platelike on either side of the canine (Fig. 35C). A finite element model of a simple plate (Fig. 36) illustrates the relationships of such a load and the resulting major stress, which is tensile and oblique to the longitudinal axis, and dips toward the position where the load is applied; a resulting crack would be normal to the direction of the maximum tensile stress and dip away from the loaded end (Fig. 36, vertical section). Similarly, the cracks near the 71.6° mode on the labial side and related cracks on the lingual side are reproducible by loads L2 in varying positions along the lower margin of the tooth and near the tip (Fig. 35A, B). Because the transverse cracks intercepting the surface on both sides of the canine usually dip away from the tip, the loading directions were probably reversed on opposite sides, with the labial loads exerted in a medial direction and the

lingual loads exerted laterally. Such loads would have been produced by pressing sometimes laterally and sometimes medially with the tips of the canines.

Conclusions

The enamel microstructure of the cheek teeth in astrapotheres is characterized by:

- vertical decussation in the inner part of the enamel
- linear boundaries of vertically decussating zones
- uniformly defined transitional zone between the vertically decussating zones
- horizontally decussating zones in the inner part of the outer enamel
- horizontal decussation angle smaller than the vertical decussation angle

The condition in astrapotheres is not distinguishable in any of these characteristics except the horizontal decussation from conditions that have been described for rhinocerotoids. The nature of the horizontal decussation in the outer enamel of rhinocerotoids, which is being studied, may make the resemblance between these groups even stronger.

The gross structures of the molars of astrapotheres, especially in the upper dentition, are remarkably similar to those of rhinocerotoids in:

- flatness of the ectoloph
- direction of the ectoloph
- shape of the ectoloph, including positions and shapes of the paracone, metacone, and metastyle
- attitude of the occlusal facet on the ectoloph
- chewing direction on the ectoloph
- shape and direction of cracks in the ectoloph enamel

The occurrence of an almost identical microstructural configuration in these two groups, an identity that cannot have occurred through a shared ancestry, is remarkable because this combination of structures has not been seen in any other group of mammals. The low probability that such a complex microstructure could have arisen independently in the two groups by chance points to a similarity of selective events during the evolution of these masticatory mechanisms.

One of these events was a flattening and joining of cusps to form narrow lophs. This event also occurred in other ungulate lineages, but in none of those that survived into the later Tertiary was there development of vertical decussation such as characterizes the rhinocerotoid and astrapothere molariform teeth. Analyses of the stresses and microstructural patterns in the other extinct taxa having vertical decussation (e.g., pyrotheres and deperetellids) and in ungulates lacking vertical decussation are needed.

The wavelike bending of HSB in the lower canine enamel of *Parastrapotherium* and the bimodal crack directions and dipping crack planes suggest that the canines were subjected to different loading conditions, lateral and medial loading near the tip and loading at the anteroventral margin a short distance back from the tip.

The differences in structure of the canine and molar enamel in these taxa appears to be a consequence of the differences in stress patterns. The distinction in the enamel structure of the upper canine of *Astrapotherium s. l.* and the lower canine of *Parastrapotherium* may be related in part to differences in form which, even under similar loads, would result in differences in stress patterns. The absence of decussation in the canine of *Astrapotherium s. l.* could be an evolutionary loss resulting from the diminished importance of crack inhibition in this larger form. The analogy to loss of enamel in the tusks of late Cenozoic proboscideans comes to mind. Resolution of this issue will require more information about the differences in structure and crack patterns of the upper and lower canines in each taxon.

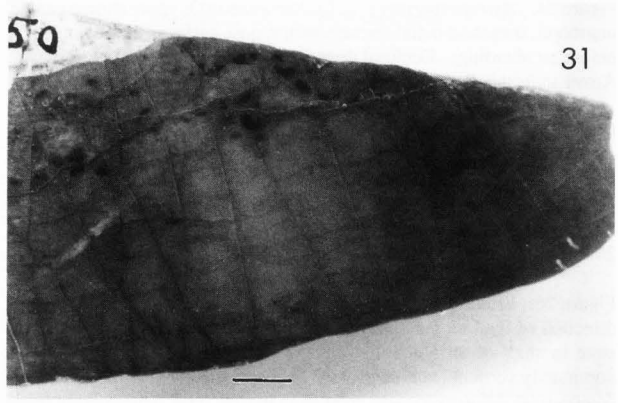

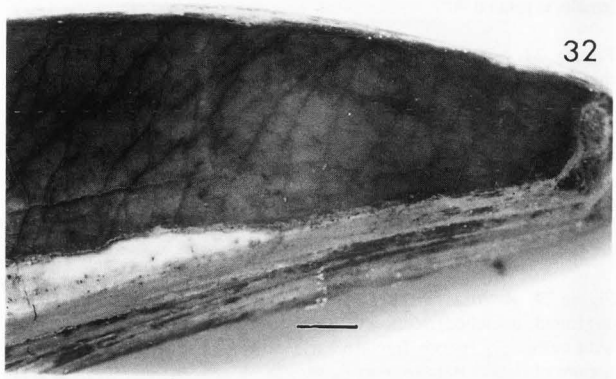

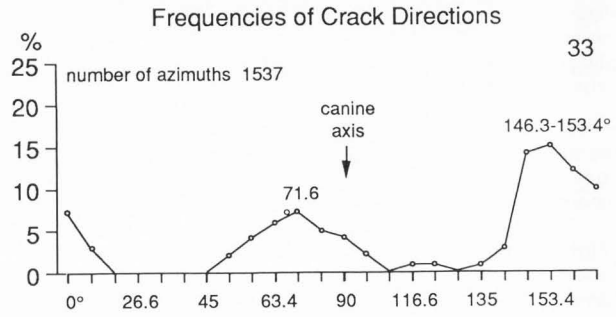

Parastrapotherium
lower canine, labial side

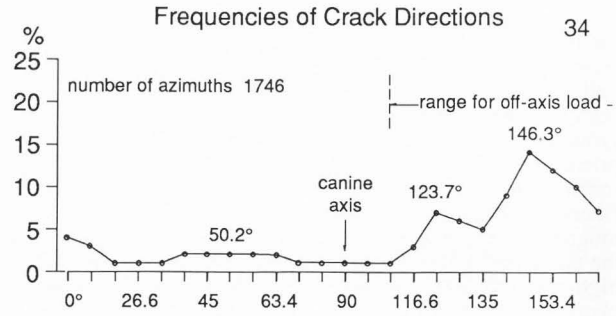

Parastrapotherium
lower canine lingual side (reversed)

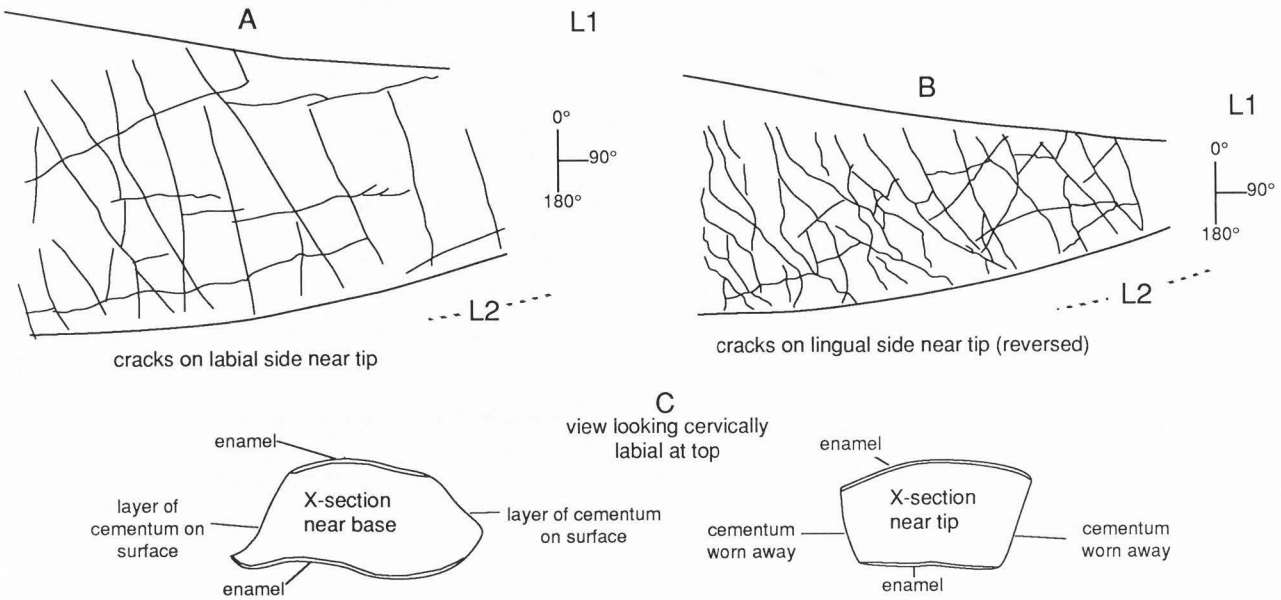

Figure 31. *Parastrapotherium*, FMNH P15050, labial view of right lower canine near tip, showing cracks in enamel. Worn tip at right. Edge at top is margin of wear surface seen in lower part of Fig. 32. Light micrograph. Bar = 5 mm.

Figure 32. *Parastrapotherium*, FMNH P15050, lingual view of canine in Fig. 31. Worn tip at right. Dentinal surface at bottom worn by tooth-tooth contact, but dentinal surface at top and enamel surface in general with extensive wear caused by contact with food or environment. Light micrograph. Bar = 5 mm.

Figure 33. Percentage frequencies of premortem crack directions in labial enamel from lower canine of *Parastrapotherium*, FMNH P15050. Fractional directions inherent in angles measured from digitized image (see Methods section for full list of directions).

Figure 34. Percentage frequencies of crack directions in lingual enamel from lower canine of *Parastrapotherium*, FMNH P15050. Most of cracks recorded are identified as premortem by dental polishing. To those have been added deep cracks that cannot be objectively identified as such, but seem to be premortem, judging from similarity of direction to premortem cracks on labial side. Azimuths near 50.2° mode derived almost entirely from deep cracks.

Figure 35. Crack patterns on labial (A) and lingual (B) enamel plates of lower canine of *Parastrapotherium* as viewed from labial side (pattern for lingual side flipped vertically); C cross-sections through canine, showing confinement of enamel to labial and lingual plates. 0°, 90°, 180° correspond to azimuth directions in Figs. 33, 34. L1 indicates position of load normal to plates accounting for major modal direction of cracks. Load at L2 (normal to plates at positions along lower margin of tusk) would account for cracks of other modal direction.

Figure 36. Directions of the major stress indicated by short solid line within each element in 3-dimensional finite element plate anchored at left end, loaded normal to surface at L1. Maximum stress is tensile. Predicted crack directions indicated by broken lines. Sectional view shows direction of major stress and dip of crack plane typical of elements in right half of model.

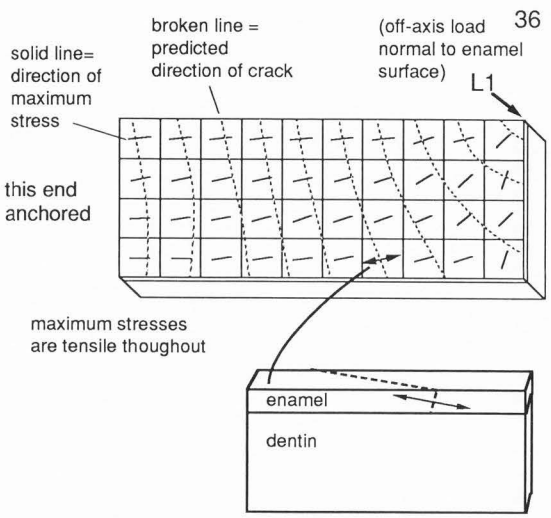

Acknowledgements

We are grateful to the following individuals who provided access to specimens in their care: WA Clemens, JH Hutchison and DE Savage (UCMP); JJ Flynn and W Turnbull (FMNH). S Johnson (UCMP) provided information derived from his recent study of astrapothere systematics. The manuscript benefitted considerably from suggestions by AW Crompton and D Stern, Harvard University; WA Clemens, UCMP; M. Fortelius, University of Helsinki; and MC Maas, Duke University. JMR is grateful to Ray Olsen and Gene Ledbury of the Boeing High Technology Center, Bellevue, WA. Mr. Ledbury's expertise was invaluable in setting up the joint SEM facility for the Department of Geological Sciences and Burke Museum at the University of Washington. Similarly, Gerry O'Loughlan, Mike Diperna, Dave Meyers, and Chris Kuyl of AMRAY Inc., and Clark Houghton of Secondary Images, Winchester, Ohio, generously provided valuable advice and assistance on various occasions. This

study was supported in part by a grant from the GSRF, University of Washington.

References

Besmann TM, Sheldon BW, Lowden RA, Stinton DP. (1991). Vapor-phase fabrication and properties of continuous-filament ceramic composites. Science 253: 1104-1109.

Borchert AM, Vecchio KS & Stein RD. (1991). The use of charging effects in Al/Al_2O_3 metal-matrix composites as a contrast mechanism in the SEM. Scanning 13:344-349.

Boyde, A. 1976. Enamel structure and cavity margins. Operative Dentistry 1:13-28.

Boyde A. 1978. Development of the structure of the enamel in the incisor teeth in the three classical subordinal groups in the Rodentia. In: Development, Function and Evolution of Teeth: P.M. Butler, K.A. Joysey, eds. pp. 43-58. Academic Press, London.

Boyde A & Fortelius M. (1986). Development, structure and function of rhinoceros enamel. Zool. Jour. Linn. Soc. 87:181-214.

Carbajal E, Pascual, R, Pinedo R, Salfity JA & Vucetich MG. (1977). Un nuevo mamífero de la Formación Lumbrera (Grupo Salta) de la Comarca de Carahuasi (Salta, Argentina). Edad y correlaciones. Publ. Mus. municip. Cien. Nat. Mar del Plata "Lorenzo Scaglia" 2:148-163.

Cifelli RL. (1983a). Eutherian tarsals from the late Paleocene of Brazil. Amer. Mus. Novitates 2761:1-31.

Cifelli RL. (1983b). The origin and affinities of the South American Condylarthra and early Tertiary Litopterna (Mammalia). Amer. Mus. Novitates 2772:1-49.

Clegg WJ, Kendall K, Alford NM, Button TW & Birchall JD. (1990). A simple way to make tough ceramics. Nature 347:455-457.

Cook, J & Gordon, JE. 1964. A mechanism for the control of crack propagation in all-brittle systems. Proc. Roy. Soc. Lond. 282A:508-520.

Crompton AW & Hiiemae K. (1969). How mammalian teeth work. Discovery 5:23-34.

Crompton AW & Sun AL. (1985). Cranial structure and relationships of the Liassic mammal *Sinoconodon*. Zool. Jour. Linn. Soc. 85:99-118.

Currey J. 1979. Mechanical properties of bone with greatly differing function. J. Biomech. 12:313-319.

Currey J. 1984. The mechanical adaptations of bones. Princeton University Press. 294 pp.

Fortelius M. (1985). Ungulate cheek teeth: developmental, functional, and evolutionary interrelations. Acta Zool. Fennica 180:1-76.

Hopson JA & Crompton AW. (1969). Origin of mammals. Pp. 15-72. In: Evolutionary Biology, Dobzhansky T, Hecht MK & Steere WC (eds). Appleton-Century-Crofts, New York. 309 pp.

Janis CM & Fortelius M. (1988). On the means whereby mammals achieve increased functional durability of their dentitions, with special reference to limiting factors. Biol. Rev. 63:197-230.

Kawai N. (1955). Comparative anatomy of the bands of Schreger. Okijimas Folia anatomica Japonica 27:115-131.

Koenigswald W von. (1980). Schmelzstruktur und Morphologie in den Molaren der Arvicolidae (Rodentia). Abh. senckenberg. naturforsch. Ges. Frankfurt 539:1-129.

Koenigswald W von. (1988). Enamel modification in enlarged front teeth among mammals and the various possible reinforcements of the enamel. In: Teeth Revisited: Proceed. of the VIIth Intern. Symp. on Dental Morphology, Paris 1986, Russell, D.E., Santoro, J.-P. & Sigogneau-Russell, D. Eds., Mém. Mus. natn. Hist. nat., Paris, (série C) 53:147-167.

Koenigswald W von, Rensberger JM & Pfretzschner HU. (1987). Changes in the tooth enamel of early Paleocene mammals allowing increased diet diversity. Nature 328:150-152.

Korvenkontio VA. (1934). Mikroskopische Untersuchungen an Nagerincisiven unter Hinweis auf die Schmelzstruktur der Backenzähne. Ann. Zool. Soc. Zool.-Bot. Fennicae Vanamo 2. 353 pp.

Lucas PW & Luke DA. (1984). Chewing it over: basic principles of food breakdown. In: Food Acquisition and Processing in Primates. Chivers DJ, Wood BA, Bilsborough A (eds). Plenum Press, New York, pp. 283-301.

Maas MC. (1986). Function and variation of enamel prism decussation in ceboid primates. Abstr., Amer. Jour. Phys. Anthr. 69:233-234.

Maas MC. (1991). Enamel structure and microwear: an experimental study of the response of enamel to shearing force. Amer. Jour. Phys. Anthr. 85:31-49.

Pfretzschner HU. (1988). Structural reinforcement and crack propagation in enamel. In: Teeth Revisited: Proceed. of the VIIth Intern. Symp. on Dental Morphology, Paris 1986, Russell, D.E., Santoro, J.-P. & Sigogneau-Russell, D. Eds., Mém. Mus. natn. Hist. nat., Paris (série C) 53:133-143.

Pfretzschner, HU. (In press a). Enamel microstructure and hypsodonty in large mammals. In: Structure, Function and Evolution of Teeth. Proc. VIIIth Intern. Symp. on Dental Morphology, Jerusalem, 1989. Freund Publ. House.

Prfetzschner HU. (In press b). Biomechanik und Schmelzmikrostruktur in den Backenzähnen von Grosssäugern. Palaeontographica A.

Rasmussen ST, Patchin, RE, Scott, DB & Heuer, AH. 1976. Fracture properties of human enamel and dentin. Jour. Dental Res. 55:154-164.

Rensberger JM. (1987). Cracks in fossil enamels resulting from premortem vs. postmortem events. Scanning Microscopy 1:631-645.

Rensberger JM. (in press). Relationship of chewing stress and enamel microstructure in rhinocerotoid cheek teeth. In: Structure, Function and Evolution of Teeth. Proceed. VIIIth Intern. Symp. on Dental Morphology, Jerusalem, 1989. Freund Publ. House.

Rensberger JM, Forstén A, & Fortelius M. (1984). Functional evolution of the cheek tooth pattern and chewing direction in Tertiary horses. Paleobiology 10:439-452.

Rensberger JM & Koenigswald W von. (1980). Functional and phylogenetic interpretation of enamel microstructure in rhinoceroses. Paleobiology 6:447-495.

Stern D, Crompton AW & Skobe Z. (1989). Enamel ultrastructure and masticatory function in molars of the American opossum, *Didelphis virginiana*. Zool. Jour. Linnean Soc. 95:311-334.

Teaford MF. (1988). A review of dental microwear and diet in modern mammals. Scanning Microscopy 2:1149-1166.

Van Valkenburgh B. (1988). Incidence of tooth breakage among large, predatory mammals. Amer. Nat. 131:291-302.

Van Valkenburgh B & Ruff, CB. (1987). Canine tooth strength and killing behavior in large carnivores. J. Zool., Lond. 212:379-397.

Young WG, McGowan M & Daley TJ. (1987). Tooth enamel structure in the Koala, *Phascolarctos cinereus*:-some functional interpretations. Scanning Microscopy 1:1925-1934.

Discussion with Reviewers

M.C. Maas: Regarding the brittleness of enamel, isn't the composite nature of enamel a feature that functions to enhance its toughness and reduce its brittleness? In other words, there are general properties of enamel, other than its structural

arrangement, which make it a strong tissue.

Authors: Yes, the behavior of enamel as a composite material enhances its toughness, but structural arrangements seem to be critical to the enhancements. Crystallites may behave as ceramic fibers in an organic matrix. Prisms behave as ceramic fibers embedded in a matrix of another ceramic, the interprismatic enamel. Although prismatic fibers and interprismatic enamel are both brittle materials, manufactured fibrous composites of two brittle materials withstand greater deformation before fracturing than either alone. In fibrous composites in general, increased toughness seems to be gained through the increased stress required to overcome the bonds and friction between the matrix and fibers running perpendicular to the crack plane during fiber pullout (Currey, 1984: Fig. 2.6), in the delamination of the fibers and matrix at the crack tip, and in overcoming the reduction in stress concentration because of blunting or branching at the crack tip (Cook & Gordon, 1964). This applies to simple prismatic enamel. HSB cause groups of prisms to behave like fibers, as indicated by the roughness of the fracture surface produced by pullout of clusters of prisms across entire HSB (Fig. 30) and by the deflecting or branching of cracks by HSB (Pfretzschner, 1988: Fig. 13). In all of the above cases, the structural organization of the enamel components with respect to the stresses seems critical to the gain in toughness. In spite of these gains, brittleness still seems to be a major factor limiting the strength of enamel. Even enamel with HSB exhibits about the lowest work to fracture among skeletal materials: 200 J/m^2 in human enamel compared to 270 for human dentin, 1710 for bovid limb bone, and 6186 for cervid antler (Rasmussen, et al., 1976; Currey, 1979).

M. Fortelius: From the point of view of evolutionary theory and systematics it might be useful to summarize the anatomical differences between astrapotheres and rhinos. Rodents and primates came into South America from the outside, and for the Paleocene the xenungulate-dinocerate relationship lurks in the background. Briefly comment on why astrapotheres are not simply displaced rhinos.

W.A. Clemens: What group included the last common ancestor of astrapotheres and rhinocerotoids? What evidence is available demonstrating that this last common ancestor lacked the specialized HSB of the astrapotheres and rhinocerotoids studied?

Authors: These questions center on the issue whether astrapotheres and rhinocerotoids might not share a common ancestry that already exhibited some specialization of the HSB shared by later members of these groups. Perhaps the most conspicuous feature indicating that astrapotheres did not derive from rhinocerotoids is the absence of a distinct hypocone in primitive members. In primitive astrapotheres (Fig. 27), unlike primitive rhinocerotoids, the hypocone is poorly developed. In the Trigonostylopidae, which have traditionally been included in the Astrapotheria, although placed in a distinct order by Simpson (1967), hypocone and metaloph are virtually absent (instead of a hypocone, there is only a slight expansion of the posterolingual cingulum). Recent studies (Carbajal et al., 1977; Cifelli, 1983a) support a close relationship between the Astrapotheria and the Trigonostylopidae. Cifelli (1983b) regarded *Trigonostylops* as the most primitive astrapothere and noted that the structural differences cited by Simpson are mainly primitive characteristics. The absence of a hypocone in *Trigonostylops* makes remote the likelihood of a relationship to the most primitive members of the Rhinocerotoidea (the Hyrachyidae), which retained the strong hypocone and adjoining metaloph of primitive perissodactyls and phenacodontid condylarths. *Hyracotherium* lacks vertical HSB (Rensberger & Koenigswald, 1980). The latest common ancestor of astrapotheres and rhinocerotoids therefore appears to have been an early Paleocene condylarth with dental characteristics more primitive than those of the phenacodontids, lacking a hypocone, lacking at least vertical HSB and possibly HSB altogether.

M. Fortelius: As far as I know, the similarity of molar enamel structure between astrapotheres and rhinoceroses extends to the level of prism pattern (both have Boyde's Pattern 3). Do you think that this is significant? To what extent would you consider the organization of apatite crystallites (as distinct from "prisms") to be important?

Authors: The differences in crystallite organization may define some broad functional differences among ungulates, especially with regard to hypsodont forms, in which the interprismatic enamel forms specialized sheets (Pfretzschner, in press a,b). Interprismatic enamel is meagerly developed in astrapotheres and rhinocerotoids. It is possible that an early difference in crystallite organization influenced the direction evolution took during later evolutionary events, but more data is needed to test this hypothesis.

W.A. Clemens: The upper and lower canines of astrapotheres differ in morphology and angle of implantation. Can you determine if the differences between the enamel microstructure of the lower canine enamel of *Parastrapotherium* and the upper canine enamel of *Astrapotherium* reflect differences in position in the dentition of the teeth compared or might differentiate canine enamel of the species?

M.C. Maas: What are the relative contributions of biomechanics and phylogeny to differences in the enamel structure of *Astrapotherium* upper canines and *Parastrapotherium* lower canines?

Authors: Until the structures in opposing canines in both taxa are studied, we can only note that the structure in the lower canine of the earlier of the two taxa, *Parastrapotherium*, combines an aspect of the structure in the upper canine of *Astrapotherium* (wavelike bending of prisms) with that in the molars of both taxa (vertical decussation). To understand the phylogenetic influence, we not only need to know the structure in the opposing canines of these taxa, but also the structure in other, preferably more primitive, astrapotheres. The differences in morphology of the upper and lower canines examined, which extends also to a difference in cross-sectional outline, the upper being subcylindrical, the lower having platelike enamel, makes the mechanics different.

M.C. Maas: Are the differences that you identify between astrapothere molars and *Parastrapotherium* canines explainable only in terms of mechanical differences in the function of the teeth, as you suggest, or is there a phylogenetic influence?

Authors: The main difference is that the HSB in the canine of *Parastrapotherium* bend whereas those in the molars of astrapotheres are straight. Both have vertical decussation. The condition in primitive ungulates seems to be straight HSB and horizontal decussation. The condition in the *Parastrapotherium* canine therefore differs from the presumed primitive condition both in bending of the decussation planes and in the attitude of these planes. The more complex HSB alignment in the canine, which gives it the ability to resist more complex stress directions, is predicted by the complex stress regime in the canines in contrast to the uniform chewing direction and stress alignment in the molars. It would be genetically more economical if the canines and molars had the same enamel microstructure, so the available evidence points to a mechanical influence. This relationship can be further tested: should it turn out that the microstructural condition in a primitive astrapothere in which the canine is still small and circular in cross-section and was loaded only at the tip has aspects of the structure in *Parastrapotherium*, that would be evidence of a phylogenetic influence dominating the mechanical relationships.

M.C. Maas. Can the authors quantify the percentage of vertical decussation and horizontal decussation? Was there any variation within a tooth? If so, could the variation be related consistently to a certain position on the tooth?

Authors. There may be variation in the development of horizontal decussation from one region of a tooth to another, but we do not have enough observational data at this time to determine whether this is true. Because of the limited material and the expectation of variation from region to region we did not feel that quantification of decussation patterns would be useful information at this time. However, we hope to pursue these problems when more data can be assembled. In the meantime, we can only note that all the material we have seen under both light and electron microscopy has had the horizontal decussation, when present, confined to an interval within the outer enamel, as shown in several of the micrographs.

Additional Reference

Simpson, GG. 1967. The beginning of the age of mammals in South America. Part 2. Bull. Amer. Mus. Nat. Hist. 137:1-260.